

Spin-related magnetoresistance of n-type ZnO:Al and Zn_{1-x}Mn_xO:Al thin films

T. Andrearczyk,^{1,*} J. Jaroszyński,^{1,†} G. Grabecki,¹ T. Dietl,^{1,2,3} T. Fukumura,⁴ and M. Kawasaki⁴

¹*Institute of Physics, Polish Academy of Science, al. Lotników 32/46, 02-668 Warszawa, Poland*

²*Institute of Theoretical Physics, Warsaw University, 00-681 Warszawa, Poland*

³*ERATO Semiconductor Spintronics Project, Japan Science and Technology Agency, al. Lotników 32/46, 02-668 Warszawa, Poland*

⁴*Institute for Materials Research, Tohoku University, Sendai 980-8577, Japan*

(Dated: June 23, 2018)

Effects of spin-orbit coupling and s-d exchange interaction are probed by magnetoresistance measurements carried out down to 50 mK on ZnO and Zn_{1-x}Mn_xO with $x = 3$ and 7%. The films were obtained by laser ablation and doped with Al to electron concentration $\sim 10^{20} \text{ cm}^{-3}$. A quantitative description of the data for ZnO:Al in terms of weak-localization theory makes it possible to determine the coupling constant $\lambda_{\text{so}} = (4.4 \pm 0.4) \times 10^{-11} \text{ eVcm}$ of the kp hamiltonian for the wurzite structure, $H_{\text{so}} = \lambda_{\text{so}} \mathbf{c}(\mathbf{s} \times \mathbf{k})$. A complex and large magnetoresistance of Zn_{1-x}Mn_xO:Al is interpreted in terms of the influence of the s-d spin-splitting and magnetic polaron formation on the disorder-modified electron-electron interactions. It is suggested that the proposed model explains the origin of magnetoresistance observed recently in many magnetic oxide systems.

PACS numbers: 72.15.Rn, 72.25.Rb, 72.80.Ey, 75.50.Pp

In the emerging field of semiconductor spintronics¹ spin-orbit and sp-d exchange interactions serve for spin manipulation in nonmagnetic and magnetic semiconductors, respectively. At the same time, these interactions limit spin coherence time in these systems. Within the standard Drude-Boltzmann theory of charge transport, spin effects contribute only weakly to the conductivity. However, electrons in doped wide band-gap semiconductors are at the localization boundary, where charge transport is strongly affected by quantum interference of both scattered waves and amplitudes of the electron-electron interaction. Accordingly, the conductance in these systems is sensitive to phase breaking mechanisms such as spin relaxation as well as to symmetry lowering perturbations such as the magnetic field and Zeeman splitting of electronic states.²

In this paper we compare magnetoresistance (MR) of non-magnetic n-ZnO and paramagnetic n-(Zn,Mn)O. In both cases MR contains positive and negative components but its overall shape and magnitude is very different, a behavior reminiscent of that observed previously for n-CdSe and n-(Cd,Mn)Se.³ A quantitative description of the results demonstrates that MR of ZnO is dominated by a destructive influence of the magnetic field on interference of scattered waves. This orbital effect produces a sizable negative MR, which below 1 mT is perturbed by the so-called antilocalization caused by a spin-orbit coupling. We determine the corresponding coupling constant and compare it to results of available first principles computations. In the case of paramagnetic n-(Zn,Mn)O, we show that MR results primarily from the influence of giant s-d spin splitting and spin scattering of bound magnetic polarons on electron-electron interactions. These effects produce large and strongly temperature dependent positive and negative MR, respectively, the latter dominating in the strongly localized regime, attained here due to strong self compensation. We argue that

our conclusions can be extended to other oxides, providing information on magnetic order and on the coupling of charge carriers to localized magnetic moments.

Our Zn_{1-x}Mn_xO thin films are grown by pulsed laser deposition technique⁴ on sapphire (0001) substrates, so that the c-axis of the wurzite structure is perpendicular to the film plane. Technological Mn contents x is 0, 0.03, and 0.07, for film thicknesses $d = 440, 310,$ and 310 nm , respectively. These Mn concentrations are consistent with SIMS as well as with the SQUID measurements.⁵ The SQUID data indicate that antiferromagnetic interactions between the nearest neighbors are relevant only. This causes a reduction of the paramagnetic spin concentration to $x_{\text{eff}} = 0.020$ and 0.038 for the two (Zn,Mn)O samples in question if the Mn magnetic moment is $5.0\mu_B$. An uniform Al doping with the concentration $x_{\text{Al}} = 0.5$ and 4% in the case of ZnO and (Zn,Mn)O, respectively, results in the high and temperature independent electron concentrations $n = 1.8, 1.4$ and $1.1 \cdot 10^{20} \text{ cm}^{-3}$, for $x = 0, 3,$ and 7% , respectively, according to Hall effect data. Transport measurements are performed in four probe geometry in a ³He/⁴He fridge down to 0.05 K, and in a ⁴He cryostat above $T > 1.5 \text{ K}$ by using a.c. lock-in technique. Two types of electric contacts have been employed. Indium contacts are easy to obtain by soldering method, but they obscure high resolution measurements when indium becomes superconducting. Accordingly, in the low temperature range we use gold spring needles as contacts.

Despite rather similar electron concentrations n , the resistivities ρ of particular samples are rather different, as shown in Fig. 1(a). The determined values of the diagonal and Hall resistivities lead to electron mobilities $\mu = 52, 14,$ and $2 \text{ cm}^2/\text{Vs}$ at 4.2 K for $x = 0, 3,$ and 7% , respectively. In order to elucidate the origin of such a strong dependence $\mu(x)$ we first evaluate the effect of alloy and spin disorder scattering as

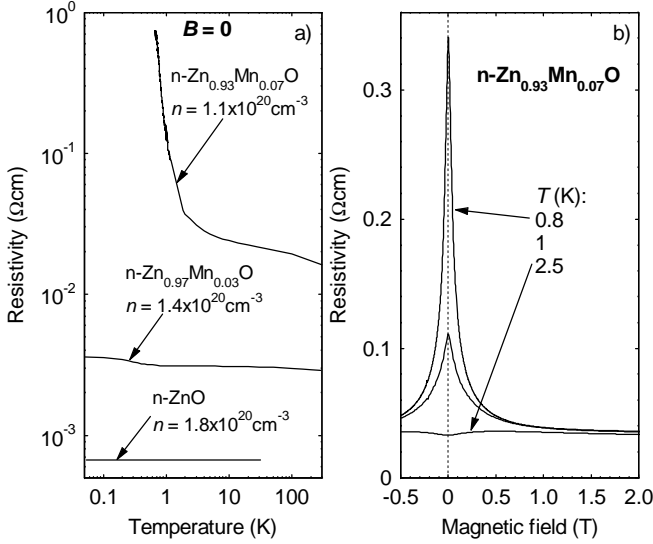


FIG. 1: Resistivity as a function of temperature (a) and magnetic field (b) for $\text{Zn}_{1-x}\text{Mn}_x\text{O}$ and $\text{Zn}_{0.93}\text{Mn}_{0.07}\text{O}$, respectively, revealing temperature dependent localization.

suming the band offset between the conduction band of wurzite MnO and ZnO and the s-d exchange energy to be $VN_o = 2 \text{ eV}$ and $\alpha N_o = 0.19 \text{ eV}$, respectively,⁶ where $N_o = 4.24 \cdot 10^{22} \text{ cm}^{-3}$ is the cation concentration in ZnO. For the effective mass $m^* = 0.3m_o$ the value of mobility limited by these scattering mechanisms is then 690 and $330 \text{ cm}^2/\text{Vs}$ for $x = 3$ and 7%, respectively, much too high to explain the experimental values.

We note, however, that the large magnitude of VN_o may account for a growing role of self-compensation with x , and elucidate why electrical activity of Al donors decreases so strongly with the Mn incorporation. Taking the static dielectric constant $\epsilon_s = 8$ and assuming that the relevant acceptor defects are singly ionized, that is that the total ionized impurity concentration is $N_{ii} = 2N_o x_{\text{Al}} - n$, we obtain from the Brooks-Herring formula $\mu_{ii} = 82, 5.0$, and $4.1 \text{ cm}^2/\text{Vs}$ for $x = 0, 3$, and 7%, respectively. These values correspond to $k_F l = 16, 0.86$, and 0.6, pointing out that the self-compensation drives the system towards Anderson-Mott localization occurring when the product of the Fermi wave vector k_F and mean free path l becomes smaller than one.² The proximity to the strongly localized regime is confirmed by a substantial temperature dependence of resistivity observed for the 7% sample. The resistivity increase is particularly strong below 1 K [Fig. 1(a)], and signals the so-called temperature dependent localization,^{3,6,7} associated with the formation of bound magnetic polarons. Colossal negative MR at low temperatures, shown in Fig. 1(b), corroborates this conclusion.

Owing to the sufficiently large experimental values of $k_F l$ in ZnO and $\text{Zn}_{0.97}\text{Mn}_{0.03}\text{O}$, we expect MR in these samples to be described by quantum corrections to conductivity in the weakly localized regime.^{2,3} Figure 2(a) depicts MR of ZnO in the field applied perpendicularly

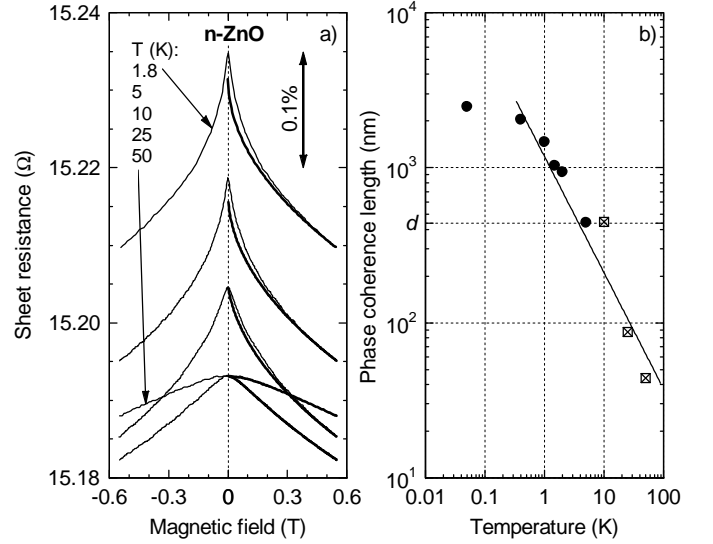


FIG. 2: Resistance changes in the magnetic field for $n\text{-ZnO}$ (thin lines) compared to calculations (thick lines) within the weak localization theory for the 3D case. For $T = 1.8$ and 5 K the phase coherence length L_φ is set to infinity, while the fitted values of L_φ at higher temperatures are plotted in (b) by squares. Dots denote L_φ determined by fitting the weak-field data presented in Fig. 3. Straight line shows the dependence $T^{-3/4}$ expected for $L_\varphi(T)$ in the 3D case.

to the film plane, that is along the c -axis. As seen, MR is negative and temperature dependent, particularly in weak magnetic fields. Such character and magnitude of MR, of the order of 0.1% at $B = 0.5 \text{ T}$, are similar to that observed for an accumulation layer on ZnO .⁸ We assign this MR to a destructive effect of the magnetic field (vector potential) on constructive interference corresponding to two time-reversal paths along the same self-crossing trajectories. Thick lines in Fig. 2(a) has been calculated within this model by using Kawabata's three dimensional (3D) formula,^{2,9} treating the phase coherence length $L_\varphi(T)$ as a fitting parameter. It is apparent, however, that the model fails to describe the data quantitatively at low temperatures and in low magnetic fields. We assign this failure to a dimensional cross-over, as according to the values of L_φ summarized in Fig. 2(b), L_φ becomes greater than the sample thickness d below 10 K.

Figure 3 presents a comparison of experimental and calculated MR of ZnO in the magnetic field below 6 mT. A characteristic positive component of MR, signaling the presence of spin-orbit scattering, is detected below 1 mT at low temperatures. Similarly to the case of $n\text{-CdSe}$,³ we link this scattering to the presence of the term $\lambda_{\text{so}} \mathbf{c}(\mathbf{s} \times \mathbf{k})$ in the kp hamiltonian of the wurzite structure, which in the employed geometry leads to the spin-orbit relaxation rates $\tau_{\text{so}x}^{-1} = \tau_{\text{so}y}^{-1} = \lambda_{\text{so}}^2 k_F^2 \tau / 12 / \hbar^2$; $\tau_{\text{so}z}^{-1} = 0$,¹⁰ where τ is momentum relaxation time. Since $L_\varphi(T) > d$ and the magnetic length $L_B = (\hbar/eB)^{1/2} = d$ at 3.4 mT we describe the data by Hikami *et al.* 2D theory,^{2,11} treating $L_\varphi(T)$ and λ_{so} as the fitting param-

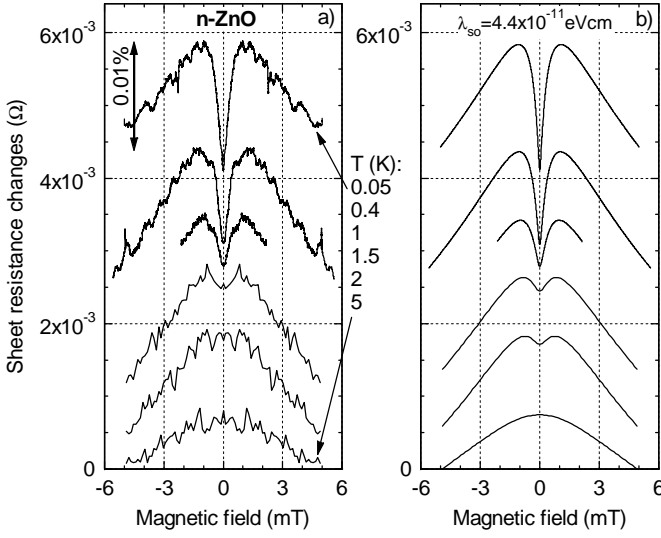


FIG. 3: Resistance changes in the magnetic field for n-ZnO (a) compared to calculations (b) within the weak localization theory for the 2D case. Curves are vertically shifted for clarity and symmetrized.

eters. As shown in Fig. 3, we obtain a quite good description of our findings with $\lambda_{so} = 4.4 \cdot 10^{-11}$ eVcm. Interestingly, the value of λ_{so} , determined within the present model with accuracy of about 10%, is by a factor two greater than that obtained by recent first principles computations.¹² In contrast, the experimental value for CdSe,^{3,13} $\lambda_{so} = (55 \pm 10) \cdot 10^{-11}$ eVcm is by a factor of two smaller than the theoretical result.¹² In any case, it is obvious that at a given electron density a dramatic reduction of τ_{so}^{-1} occurs on going from heavier CdSe to lighter ZnO. Finally, we note that according to Fig. 2(b), $L_{\varphi}(T) \sim T^{-3/4}$ down to 0.5 K, as expected for the phase breaking by electron-electron collisions in disordered 3D systems.² Since $L_T = (\hbar D/k_B T)^{1/2} = d$ at 50 mK, we assign a weaker temperature dependence at low temperatures to an onset of the dimensional cross-over, as in the 2D case $L_{\varphi}(T) \sim T^{-1/2}$.² However, at this stage, we cannot exclude perturbation effects of stray fields or noise heating at the lowest temperatures, which may affect the determined values of $L_{\varphi}(T)$.

We now turn to MR found for the films of paramagnetic (Zn,Mn)O, shown in Fig. 4. A competition between positive and negative contributions to MR is clearly visible. Despite that the overall shape of MR is similar to that n-ZnO, its huge magnitude as well as the field and temperature dependencies indicate that effects brought about by the presence of the Mn spins dominate. Actually, it has been shown previously^{3,6,14,15} that giant spin-splitting of band states in diluted magnetic semiconductors affects considerably quantum correction to the conductivity associated with the disorder modified electron-electron interactions.² This results in positive MR,² if the Mn ions are not already spin-polarized in the absence of the magnetic field. Furthermore, the spin-

splitting lead to a redistribution of the electrons between spin subbands, which diminishes localization by increasing the carrier kinetic energy.¹⁶ In our case, however, the spin-splitting is more than ten times smaller than the Fermi energy, which makes this mechanism of a minor importance. We rather assign the negative component of MR to an enhancement of spin-disorder scattering associated with the formation of bound magnetic polarons on approaching the strongly localized regime,^{3,6} though quantitative theory of the effect has not yet been elaborated. In line with this model, negative MR becomes stronger with decreasing temperature and increasing Mn content.

We execute MR calculations for (Zn,Mn)O with no fitting parameter taking into account both single-electron and many-body quantum effects in the weakly localized regime, $k_F l \gg 1$.² Because of smaller magnitude of diffusion constant in (Zn,Mn)O comparing to ZnO, we employ the 3D formulae.² The spin-splitting of the conduction band contains the Zeeman term $g\mu_B H$, where $g = 2.0$ in ZnO, and the s-d contribution $x_{eff}\alpha N_o S B_S(T, H)$, where the numerical values of x_{eff} and αN_o have been given above and, in the temperature range of interest here, B_S is the paramagnetic Brillouin function for $S = 5/2$. The parameter describing the magnitude of electron-electron interaction in the triplet channel is taken as $F_{\sigma} = 2g_3 = 1$. Furthermore, for $\tau_{\varphi}(T)$ we adopt the values obtained for ZnO. As shown in Figs. 4(a,b), the calculation for the 3% sample reproduces well the competition between negative and positive contributions to MR at high temperatures. At lower temperatures, however, only positive component is properly described in the range of the weak fields. In high fields and at low temperatures, in turn, we deal with an additional negative contribution, which is too large to be explained by the employed weak-localization theory. We regard this effect as a precursor of the polaron formation. This situation is even more marked for $x = 7\%$ sample, for which the comparison between measured and calculated MR is depicted in Figs. 4(c,d). We note that $k_F l \approx 2.4$ and $k_F l \approx 0.2$ for the $x = 3\%$ and $x = 7\%$ samples, respectively, which means that the 7% sample is in the strongly localized regime, for which polaron effects should be particularly important.

In summary, we have determined the magnitude of spin-orbit relaxation time of electrons in ZnO by describing quantitatively high-resolution low-temperature MR measurements in terms of quantum corrections to the conductivity of disordered systems. Within our interpretation, this spin scattering rate is proportional to the square of the coupling constant between the spin and momentum, in contrast to the corresponding band splitting that is linear in λ_{so} . Accordingly, wide-band gap semiconductors for which λ_{so} is small, appear to be particularly suitable for spin manipulation by spin-orbit effects. A small magnitude of λ_{so} makes also the corresponding MR to become dominated, in rather weak magnetic fields, by MR associated with the influence of

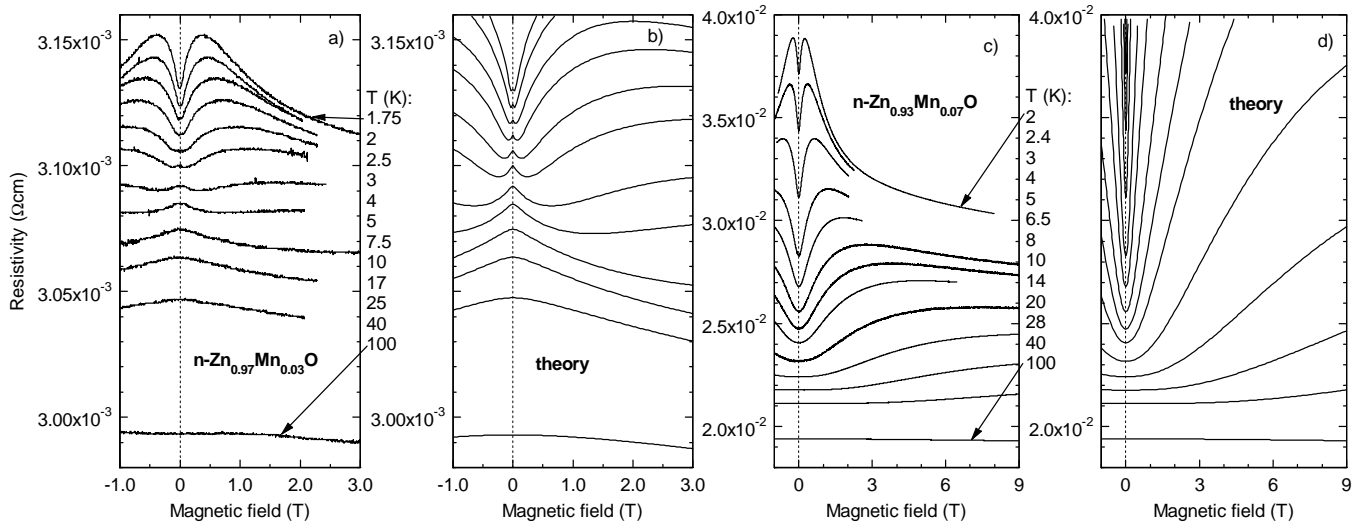


FIG. 4: Measured (a,c) and calculated with no adjustable parameter (b,d) resistivity changes in the magnetic field for $n\text{-Zn}_{0.97}\text{Mn}_{0.03}\text{O}$ (a,b) and $n\text{-Zn}_{0.93}\text{Mn}_{0.07}\text{O}$ (c,d). Weak localization theory takes into account effects of the magnetic field on interference of scattered waves and of the spin-splitting on disorder-modified electron-electron interactions but neglects effects associated with the formation of magnetic polarons, which are thought to result in negative magnetoresistance at low temperatures.

the vector potential on interference of self-crossing trajectories. Interestingly, this orbital effect makes *negative* MR to be a characteristic feature of *non-magnetic* semiconductors, while the presence of a giant spin-splitting, specific to diluted magnetic semiconductors in a paramagnetic phase, gives rise to large positive MR. This is in contrast to both diluted magnetic metals and magnetic semiconductors in the strongly localized regime, in which negative, not positive, MR points to the presence of a coupling between localized spins and charge carriers. In diluted magnetic semiconductors at the localization boundary, there is a coexistence of positive and negative MR caused by the spin-splitting and the formation of

bound magnetic polarons, respectively. The latter takes over at low temperatures and to our knowledge has not yet been described theoretically. Importantly, the model of MR invoked here appears to explain qualitatively the findings reported previously for $(\text{Zn,Mn})\text{O}$,⁴ $(\text{Zn,Co})\text{O}$,¹⁷ $(\text{Zn,Fe})\text{O}$,¹⁸ $(\text{Sn,Mn})\text{O}_2$,¹⁹ $(\text{Ti,Co})\text{O}_2$,²⁰ to quote only a few examples. In particular, the presence of sizable positive MR, suggests that the band splitting vanishes in the absence of an external magnetic field.

We thank Hideo Ohno and Maciej Sawicki for valuable discussions. This work was partly supported by PBZ/KBN/044/P03/2001 Grant and ERATO Semiconductor Spintronics Project.

* andrea@ifpan.edu.pl

† present address: National High Magnetic Field Laboratory, Florida State University, Tallahassee, Florida 32310

¹ S.A. Wolf *et al.*, Science **294**, 1488 (2001); T. Dietl, Acta Phys. Polon. A **100** (suppl.), 139 (2001); H. Ohno *et al.*, JSAP International **5**, 4 (2002); I. Žutić *et al.*, Rev. Mod. Phys. **76**, 323 (2004).

² B.L. Altshuler, A.G. Aronov in: *Electron-Electron Interactions in Disordered Systems*, edited by A.L. Efros and M. Pollak (North Holland, Amsterdam, 1985) p. 1; H. Fukuyama, *ibid.*, p. 155; P.A. Lee and T.V. Ramakrishnan, Rev. Mod. Phys. **57**, 287 (1985).

³ M. Sawicki *et al.*, Phys. Rev. Lett. **56**, 508 (1986).

⁴ T. Fukumura *et al.*, Appl. Phys. Lett. **75**, 3366 (1999).

⁵ M. Sawicki *et al.*, unpublished.

⁶ T. Dietl in: *Handbook on Semiconductors*, edited by T.S. Moss, vol. **3B** (North Holland, Amsterdam, 1994) p. 1251.

⁷ D. Ferrand *et al.*, Phys. Rev. B **63**, 085201 (2001).

⁸ A. Goldenblum *et al.*, Phys. Rev. B **60**, 5832 (1999).

⁹ A. Kawabata, J. Phys. Soc. Jpn. **49**, 628 (1980).

¹⁰ B.L. Altshuler *et al.*, in *Quantum Theory of Solids*, edited by I.M. Lifshits (Mir Publishers, Moscow, 1982), p.130, and references therein.

¹¹ S. Hikami *et al.*, Prog. Theor. Phys. **63**, 707 (1980).

¹² L.C. Lew Yan Voon *et al.*, Phys. Rev. B **53**, 10703 (1996).

¹³ M. Dobrowolska *et al.*, Phys. Rev. B **29**, 6652 (1984).

¹⁴ I.P. Smorchkova *et al.*, Phys. Rev. Lett. **78**, 3571 (1997).

¹⁵ T. Andrearczyk *et al.*, Phys. E **12**, 361 (2002).

¹⁶ H. Fukuyama and K. Yoshida, J. Phys. Soc. Japan **46**, 1522 (1979).

¹⁷ Jae Hyun Kim *et al.*, Phys. B **327**, 304 (2003).

¹⁸ S.-J. Han *et al.*, Appl. Phys. Lett. **81**, 4212 (2002).

¹⁹ H. Kimura *et al.*, Appl. Phys. Lett. **80**, 94 (2002).

²⁰ S.R. Shinde *et al.*, Phys. Rev. B **67**, 115211 (2003).